ISSN (Print) 1226-1750
ISSN (Online) 2233-6656
Journal of Magnetics 22(4), 596-604 (2017) https://doi.org/10.4283/JMAG.2017.22.4.596

Characteristic Analysis and Comparative Investigation on Permanent Magnet Synchronous Machines considering Operating Conditions

Yu-Seop Park*

Department of Electrical Engineering, Korea National University of Transportation, Chungju 27469, Republic of Korea

(Received 25 September 2017, Received in final form 11 December 2017, Accepted 16 December 2017)

This paper deals with the comparative investigation on an interior permanent magnet synchronous machine (IPMSM) and a surface-mounted permanent magnet synchronous machine (SPMSM) considering operating conditions, and finite element method (FEM) is employed to analyze their electromagnetic field characteristics. For the reasonable comparison, those machines have identical machine size and equivalent circuit parameters, such as induced voltage and resistance, and one of the analysis models is manufactured for the experimental verification. From the no-load and load test, the induced voltage and phase current are measured, and the validity of analysis results are demonstrated by showing well corresponded results. In addition, since the phase current contains harmonic components, they are considered in the power loss characteristic analysis by considering operating conditions to investigate their influence on machine performance. In this study, the SPMSM shows relatively better core loss and rotor loss characteristics compared to IPMSM when the machines are operated in high rotational speed condition.

Keywords : IPMSM, operating mode, SPMSM

1. Introduction

Recently, due to its higher energy density and superior performance, permanent magnet synchronous machines (PMSMs) are widely addressed in plenty of previous studies with different machine types for their appropriate applications [1-3]. Although the types of the machines can be various, they are largely divided into interior PMSM (IPMSM) and surface-mounted PMSM (SPMSM) according to the position of PMs in their rotor. Since each machine type has their own benefits, the designers consider the specific applications and the required machine performance to attract the advantage of those machines. On the other hand, to analyze the electromagnetic field characteristics and to achieve the performance improvement, the related studies on both machines have been actively performed. The authors in [4] addressed the characteristics of the IPMSM with fractional-slot concentrated windings in the stator and the V-type PM arrangement in the rotor structure. By considering rotor topology, deep insights on their machine performance were comparatively analyzed while the study showed the method to reduce the demagnetization. On the other hand, the study presented in [5] investigated the effects of winding types on the IPMSM, iron loss and rotor loss characteristics were compared by showing the benefits of their multilayer winding.

On the other hand, according to their industrial applications, the machines may be operated in motoring mode or in generating mode. Differently from the motoring mode, when the machines are in generating mode, the comparison of IPMSM and SPMSM under the identical mechanical size condition and machine parameters by considering leading and lagging current has been seldom performed. For the stable operation of the system in which they are employed, the influence of the operating conditions on the machines is highly required to be addressed so that the best determination of the machine type can be made. Therefore, based on finite element method (FEM), this study addressed the comparative characteristic analysis of the IPMSM and the SPMSM under identical size condition and equivalent circuit parameters, and investigation on their electromagnetic field characteristics and the power losses is performed with experimental verification. In this study, the analysis models are introduced with the specific values of their design

*Corresponding author: Tel: +82-43-841-5148
Fax: +82-43-841-5140, e-mail: yspark@ut.ac.kr

parameters in chapter II, and the electromagnetic field analysis results are compared according to the machine types. On the other hand, in chapter III, one of the analysis machines is manufactured, and the relevant experimental set is constructed to validate the analysis results. In addition, the measured current is applied to the power loss characteristic analysis so that the proper conclusion can be made from the comparative investigation.

2. Comparative Characteristic Analysis on Permanent Magnet Synchronous Machines based on Electromagnetic Field Analysis

2.1. Analysis Models

First of all, in this study, for the reasonable comparison, the machine size of the analysis models, such as outer diameter, mechanical air-gap and stack length are limited to be identical. In other words, Fig. 1 shows two machines according to rotor topology addressed in this study, and they have identical stator structure with copper coil windings while each rotor has been designed to have almost identical induced voltage values in no-load condition. Furthermore, in their stator core, three phase and concentrated windings are placed with Y-connection, and the SPMSM has a sleeve in its rotor to prevent the PMs from detached under high speed operating conditions. As shown in the figures, the number of poles of both machines is six by applying N42SH, which is the rare- earth PM, proper pole arc ratio is applied for low cogging torque and sinusoidal induced voltage waveform. In addition, since the material of the sleeve is Inconel 718, its magnetic influence on the machine is very low while the magnetic air-gap of the SPMSM is relatively larger than that of the IPMSM. More details of their design specifications are presented in Table 1. As mentioned above, those machines have almost identical value of induced voltage in no-load condition. Since the SPMSM has relatively larger magnetic air-gap than the IPMSM, more volume of PMs was required to meet the value of induced

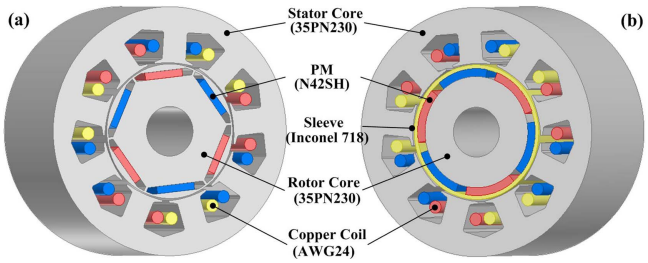

Fig. 1. (Color online) Analysis models for electromagnetic field characteristic analysis according to operating conditions with identical stator structure: (a) IPMSM, (b) SPMSM.

Table 1. Design Specification of Analysis Models.

Specification	Unit	IPMSM	SPMSM
Rated Power	W	230	
Rated Torque	Nm	1.1	
Rated Speed	rpm	6,000	
Rated Current	A	1.5	
Number of Poles	-	6	
Number of Slots		9	
Outer Radius of Stator	mm	50	
Inner Radius of Stator	mm	27.5	
Outer Radius of Rotor	mm	27	
Inner Radius of Rotor	mm	10	
Thickness of Sleeve	mm	-	1.5
Stack length	mm	55	
Mechanical Air-gap	mm	0.5	
PM Thickness	mm	3	3.2
PM Volume	mm^3	15308.7	22024.2
PM Material	-	N42SH	
Number of Coil Turns	turns	84	
Induced Voltage (1,000rpm)	V_{max}	31.3	31.8
Line-to-Line Resistance	ohm	2.5	
Winding Connection	-	Y	

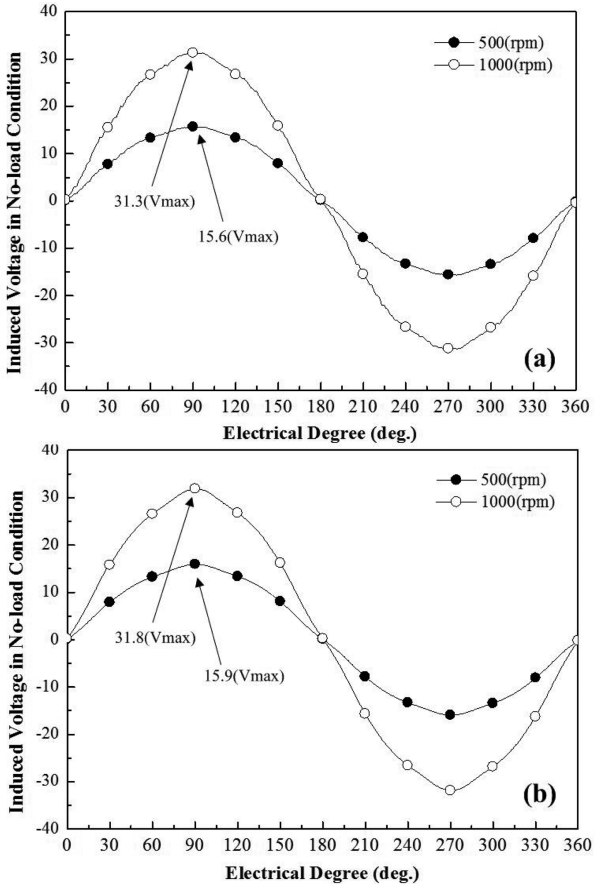

Fig. 2. Induced voltage in no-load condition according to rotational speed conditions (line to line): (a) IPMSM, (b) SPMSM.

voltage as provided in the Table 1. In other words, Fig. 2 shows the analyzed induced voltage of both machines according to the rotational speed without any current in the stator. As shown in the figures, the speed condition 500(rpm) and 1,000(rpm) are analyzed, and the line-to-line voltage values are presented for later experimental verification. In the figures, although a bit little difference can be found, it is considered that they are well corresponded to be reasonable comparison.

2.2. Flux Density Distribution according to Operating Conditions

In this paper, as presented in Fig. 3 and Fig. 4, the flux density characteristics of each machine in air-gap are analyzed according to power factor when they are in generating mode. In those figures, it can be known that the influence of the load conditions on the IPMSM is higher than that of the SPMSM. In other words, the difference in A and B region is visible when it comes to the IPMSM, but the SPMSM shows almost similar characteristics regardless of the power factor variation.

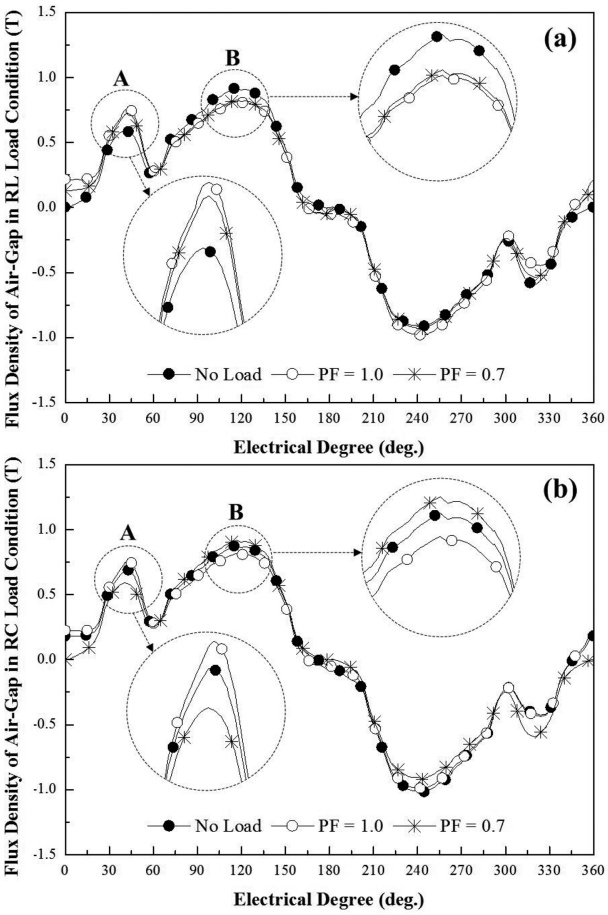

Fig. 3. Flux density of IPMSG in air-gap according to power factor: (a) leading current, (b) lagging current.

This phenomenon can be explained by the flux density by their armature current presented in Fig. 5. For this analysis, the PMs in both machines were removed, and the analysis was performed with 1(A_{rms}) current condition. As easily

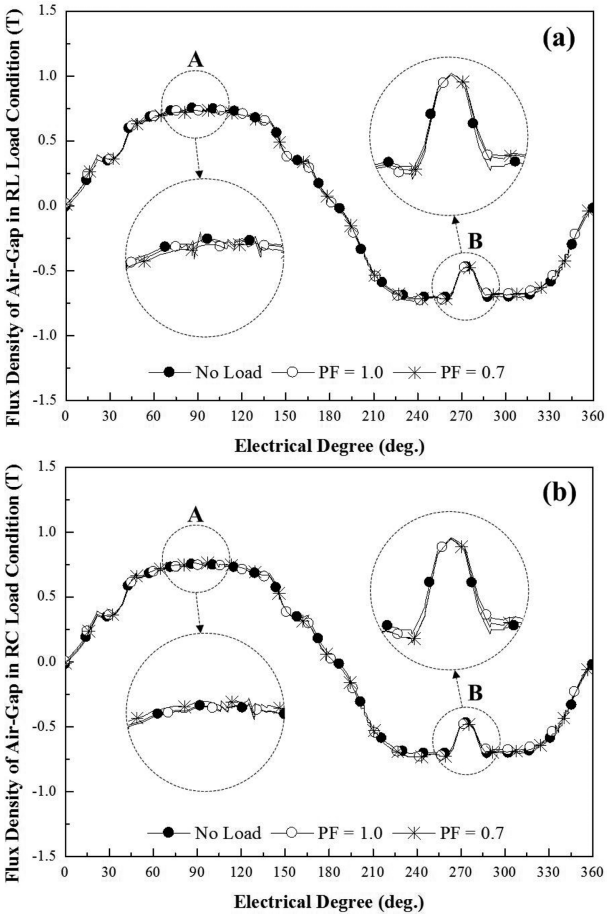

Fig. 4. Flux density of SPMSG in air-gap according to power factor: leading current, (b) lagging current.

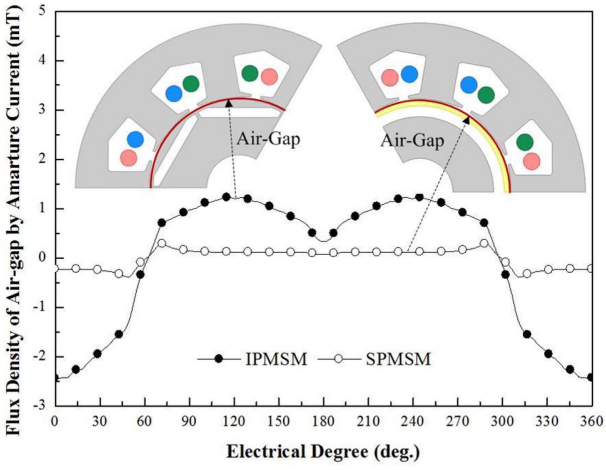

Fig. 5. (Color online) Flux density of each machine by armature current in rotor (1A_{rms}).

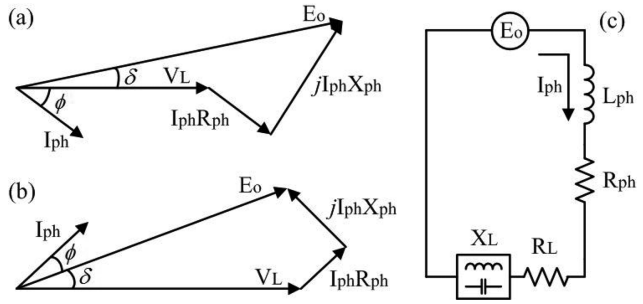

Fig. 6. Vector diagram and equivalent circuit of PM machines in generating mode: (a) lagging current, (b) leading current, (c) equivalent circuit.

found in the figure, the value of flux density of the armature current of the SPMSM is much lower than the IPMSM, and it is resulted from relatively larger magnetic air-gap.

On the other hand, the vector diagram according to operating conditions and the equivalent circuit of the machines are presented in Fig. 6. In the figure, E_o, V_L, I_{ph}, and X_{ph} are induced voltage, load voltage, phase current and reactance while L_{ph}, R_{ph}, R_L and X_L are phase inductance, phase resistance, load resistance and load reactance, respectively. Based on the derived machine parameters, such as induced voltage, resistance and inductance, the output voltage and current can be derived, and the figures in Fig. 7 and Fig. 8 respectively present the achieved output voltage and current characteristics of both machines according to operating conditions. As shown in the figure, the operating conditions are divided into RL load and RC load conditions to vary the power factor with leading and lagging current. As confirmed in the figure, the machines show almost identical output characteristics in terms of the values of the voltage and current, so their comparison can be reasonable in that they have very similar equivalent circuit parameters under identical machine size condition except for their different rotor topology. On the other hand, in Fig. 9, the analyzed voltage and current waveforms are presented according to machine types when the power factor is 0.7 with leading current. As shown in those figures, the harmonic compo-

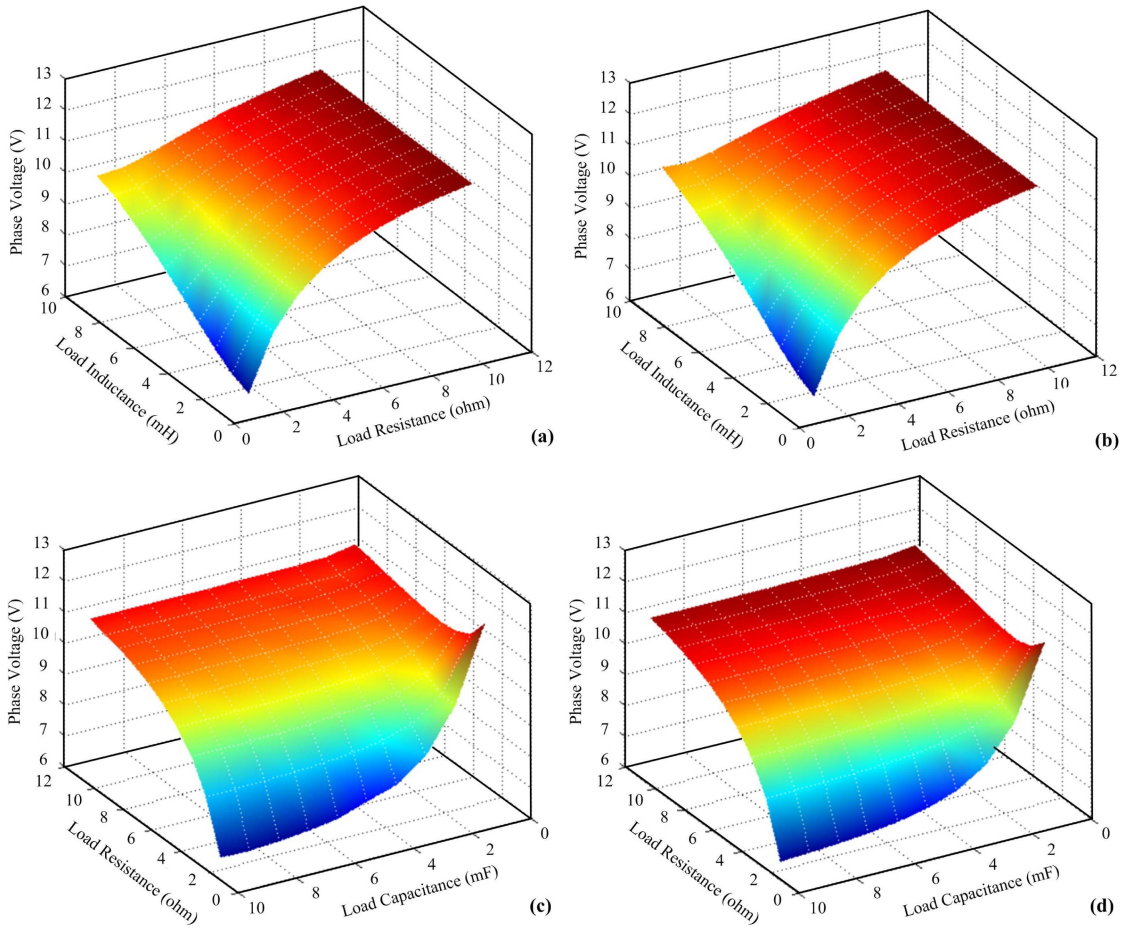

Fig. 7. (Color online) Output phase voltage characteristics of analysis models according to operating conditions: (a) IPMSM with RL load, (b) SPMSM with RL load, (c) IPMSM with RC load, (d) SPMSM with RC load.

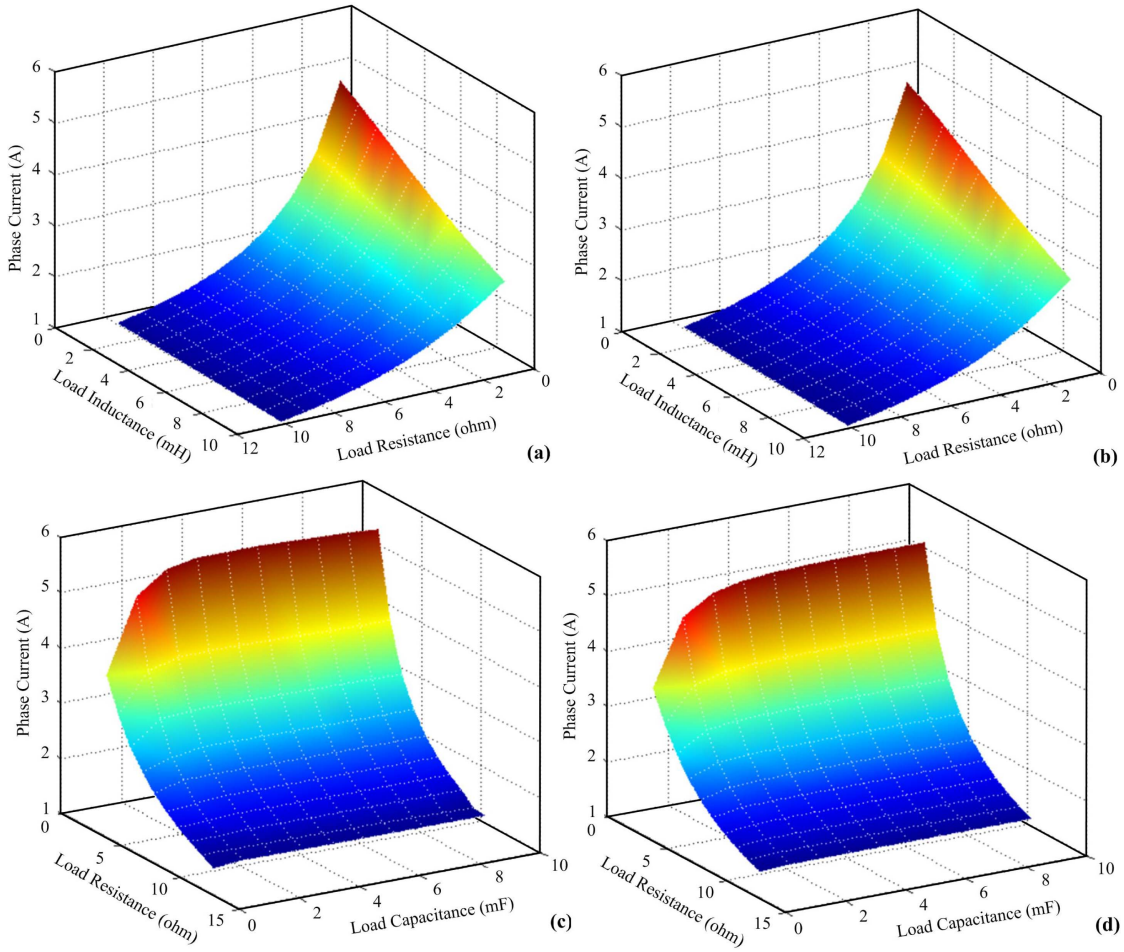

Fig. 8. (Color online) Phase current characteristics of analysis models according to operating conditions: (a) IPMSM with RL load, (b) SPMSM with RL load, (c) IPMSM with RC load, (d) SPMSM with RC load.

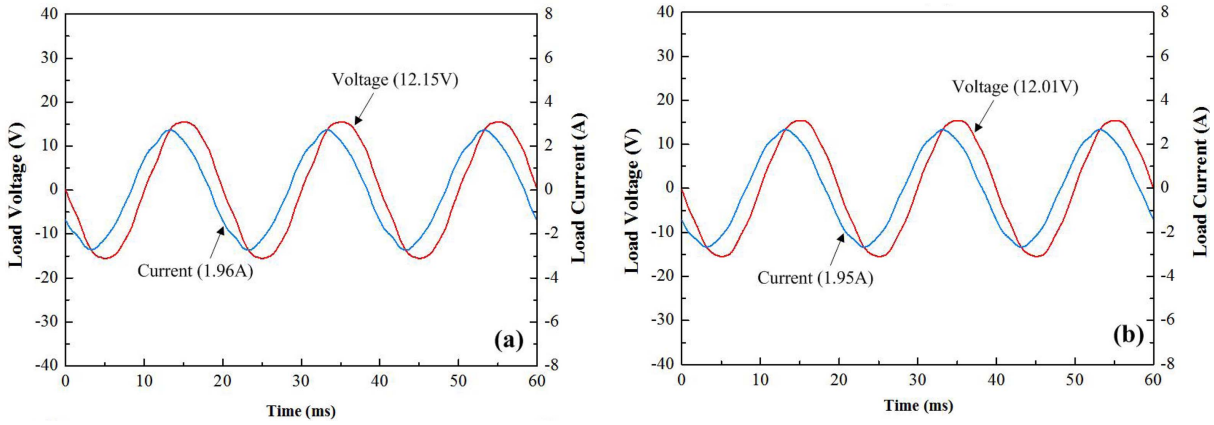

Fig. 9. (Color online) Analyzed output voltage and current characteristics in RC load condition (speed = 1,000(rpm), power factor = 0.7): (a) IPMSM, (b) SPMSM.

nents are confirmed in the current, and they can have high influence on the machine performance. In other words, as discussed in [6], since the power loss equations are expressed by considering the harmonic order, their consideration will make the analysis results of power loss more accurate.

3. Experimental Verification and Investigation on Performance of IPMSM and SPMSM according to Operating Conditions

3.1. Experimental Set with Manufactured Machine

In this paper, for the experimental verification, a manufactured IPMSM, which is one of the analysis models, is employed. As presented in Fig. 10, the manufactured machine and the constructed experimental set are presented. As shown in the figure, the experiment can be performed according to the operating mode, such as the generating mode and the motoring mode. For the generating mode, the manufactured IPMSM is directly connected to an induction motor with the operating inverter for mechanical input power while the three phase coil windings of the IPMSM are connected to a load bank. One the other hand, for the motoring mode, the IPMSM is controlled by the space vector pulse width modulation (SVPWM) inverter, while the induction motor is operated as a load motor. In this study, for the comparison of power loss characteristics, the measured current in both the generating mode and the motoring mode was measured from experiment.

First of all, with the constructed experimental set, the induced voltage is measured according to rotational speed conditions, and the experimental waveforms of the line-to-line induced voltage are presented in Fig. 11. As can be confirmed by comparing the figures in Fig. 2 and Fig. 11, they are very well corresponded each other by demonstrating the validity of the analysis method.

3.2. Current Characteristics according to Operating Mode

As mentioned above, the machines can be operated in both generating mode and motoring mode according to their applications. When it comes to motoring mode, the phase current can be influenced by the operating inverter with control technique while the machine characteristics in generating mode has relationship with load conditions. With the manufactured IPMSM in Fig. 10, the machine

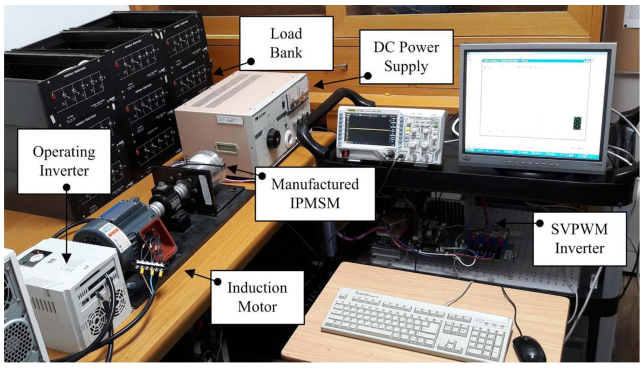

Fig. 10. (Color online) Manufactured IPMSM and constructed experimental set with SVPWM Inverter for generating and motoring mode.

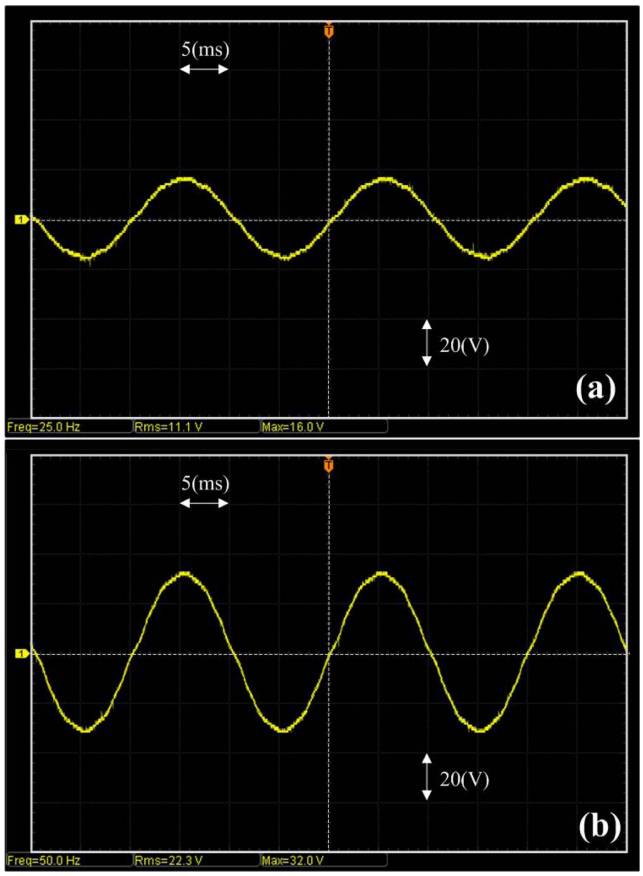

Fig. 11. (Color online) Measured induced voltage of IPMSM according to rotational speed condition (line-to-line): (a) 500(rpm), (b) 1,000(rpm).

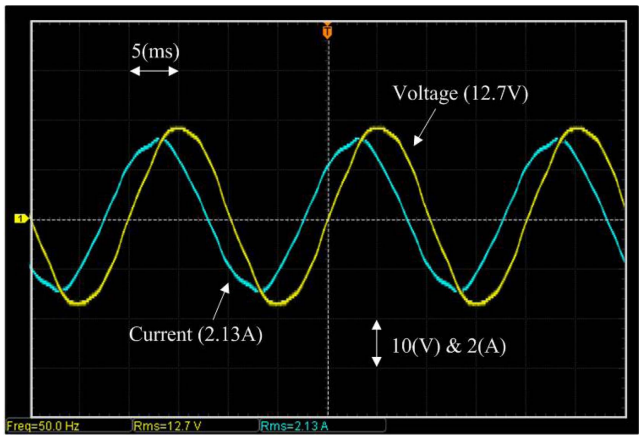

Fig. 12. (Color online) Measured output voltage and current characteristics of IPMSM in RC load condition of generating mode (speed = 1,000(rpm), power factor = 0.7).

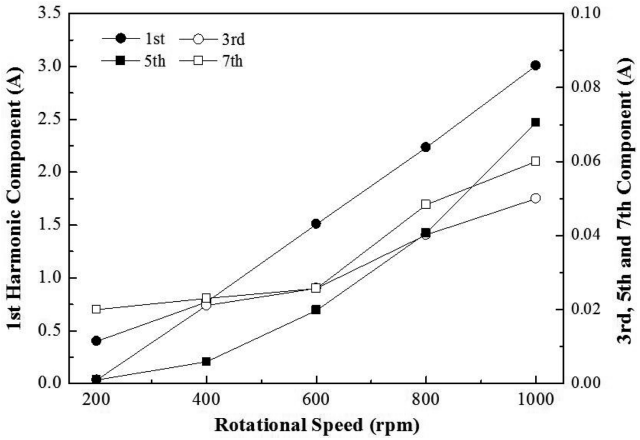

Fig. 13. FFT results of measured current of IPMSM according to rotational speed condition.

test in generating mode is firstly performed. In this experiment, the speed of the induction motor for the mechanical input power was controlled to be 1,000(rpm) while the load voltage and leading phase current are measured as shown in Fig. 12. Compared to Fig. 9, the analyzed results are also validated as well by showing well corresponded waveform. In addition, as the FFT results of the measured current in Fig. 13, each harmonic component is increased according to the rotational speed. In particular, it is known that the fifth harmonic component has high influence on rotor loss [7]. Therefore, for the accurate analysis of power losses, those harmonics are considered in this study.

On the other hand, to compare the machine performance, the manufactured IPMSM is also operated in motoring mode. In this case, as shown in Fig. 10, the speed of IPMSM is controlled by the integrated SVPWM inverter while the induction motor is operated as a load motor having its torque to inverse direction. In addition, for the similar condition to the generating mode, the d- and q-current are controlled by the SVPWM inverter. In Fig. 14, the measured reference voltage and the leading current of the IPMSM is presented. In the figure, the reference voltage is the RC-filtered PWM signal by converting the digital signal to the analog signal. In the control system, since the reference voltage and induced phase voltage is matched as shown in Fig. 14, the angle difference between the phase current and the induced voltage can be confirmed. In addition, in Fig. 15, the FFT results of the measured phase current in both generating mode and motoring mode are compared. As mentioned above, the power losses have very close relevance to those harmonics, and it can be confirmed that the motoring mode results relatively higher power losses.

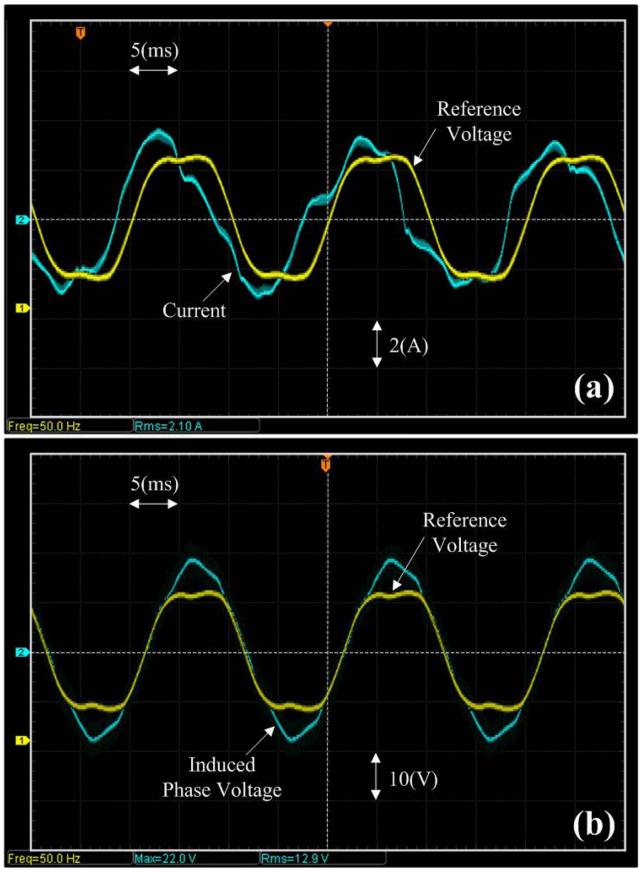

Fig. 14. (Color online) Measured machine characteristic in motoring mode : (a) phase current and RC-filtered PWM signal, (b) induced phase voltage at 1,000(rpm).

3.3. Power Loss Characteristics

The power losses of the PM machines can be various, and they are largely divided into electrical and mechanical losses. Since the mechanical losses of the low power machines are negligible, the electrical losses are dominant in the analysis models. As presented in previous study [6], the electrical power losses can be derived by (1)-(2). In those equations, l is the order of harmonic component and Q is the magnetic behavior constant. In other words, Q=1 is the alternating filed and Q=2 is the rotating field. In addition, k_h, k_e and k_{ex} are respectively the constant of hysteresis, eddy current and excess loss. On the other hand, the rotor loss is derived by FEM based on measured current so that the influence of the harmonics is considered.

$$P_{copper} = 3R_s \sum_{l=1}^{\infty} I_l^2 \tag{1}$$

$$P_{core} = \sum_{l=1}^{\infty} Q_l (k_{hl} f_l B_l^n + k_{el} f_l^2 B_l^2 + k_{al} f_l^{1.5} B_l^{1.5}) \tag{2}$$

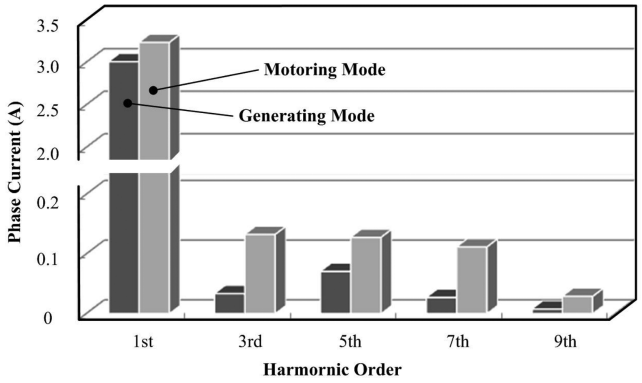

Fig. 15. FFT results of measured current according to operating mode.

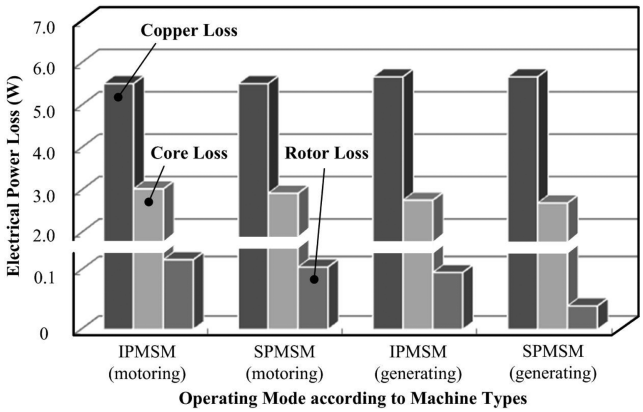

Fig. 16. Power loss characteristics according to operating mode by applying the current in Fig. 12 and Fig. 14.

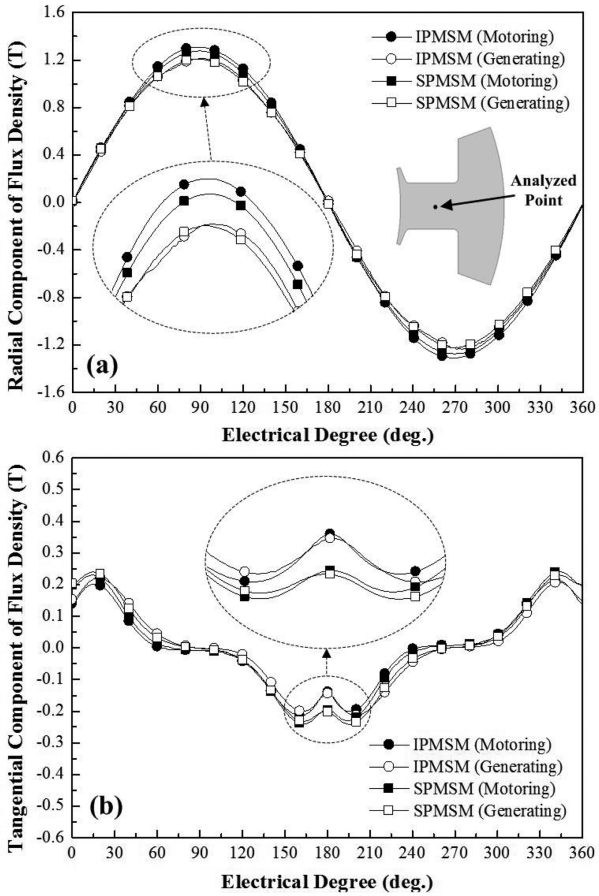

Fig. 17. Each component of flux density based on measure current according to machine types and operating mode: (a) radial component, (b) tangential component.

At first, the power losses according to the operating mode and the motor types are presented in Fig. 16, and it can be noticed that the motoring mode results more core loss and rotor loss than generating mode due to the harmonic components presented in Fig. 15. Besides, as shown in Fig. 17, the increased flux density is confirmed in the stator core when the machine is being operated in motoring mode. One the other hand, when it comes to machine types, the visible difference of the rotor loss can be found from the SPMSM in generating mode. It is considered that the larger mechanical air-gap of the SPMSM reduced the influence of harmonics on the surface of the PMs. The core loss values according to operating mode have minor difference in spite of the higher harmonics of the motoring mode. On the other hand, when it comes to rotor loss, the fifth harmonic component has much more influence on rotor loss than the others as mentioned in the previous study. It is considered that the visible difference of the rotor loss was caused by the fifth component.

On the other hand, the analysis conditions are under low speed condition of 1,000(rpm), it is necessary to confirm their characteristics according to rotational speed. Since the validity of the current characteristics is demonstrated, the reliable power losses can be predicted while the machine speed is being increased. In Fig. 18, the power losses according to the rotational speed are compared while the results are derived in generating mode. Here, the maximum operating speed is 10,000(rpm).

As can be confirmed in the figures, the losses have minor difference in low speed range, but the high speed condition results visibly different values. When it comes to copper loss, the SPMSM has much higher value compared to the IPMSM. Although the machines are designed to have identical induced voltage in no-load condition, the SPMSM has relatively higher values. This results more copper loss values in high speed region. On the other, the IPMSM has more core loss values, and this is caused by the higher magnetic flux density and its harmonics as presented in the figure. Furthermore, in those machines, the rotor loss is not negligible, and IPMSM shows almost

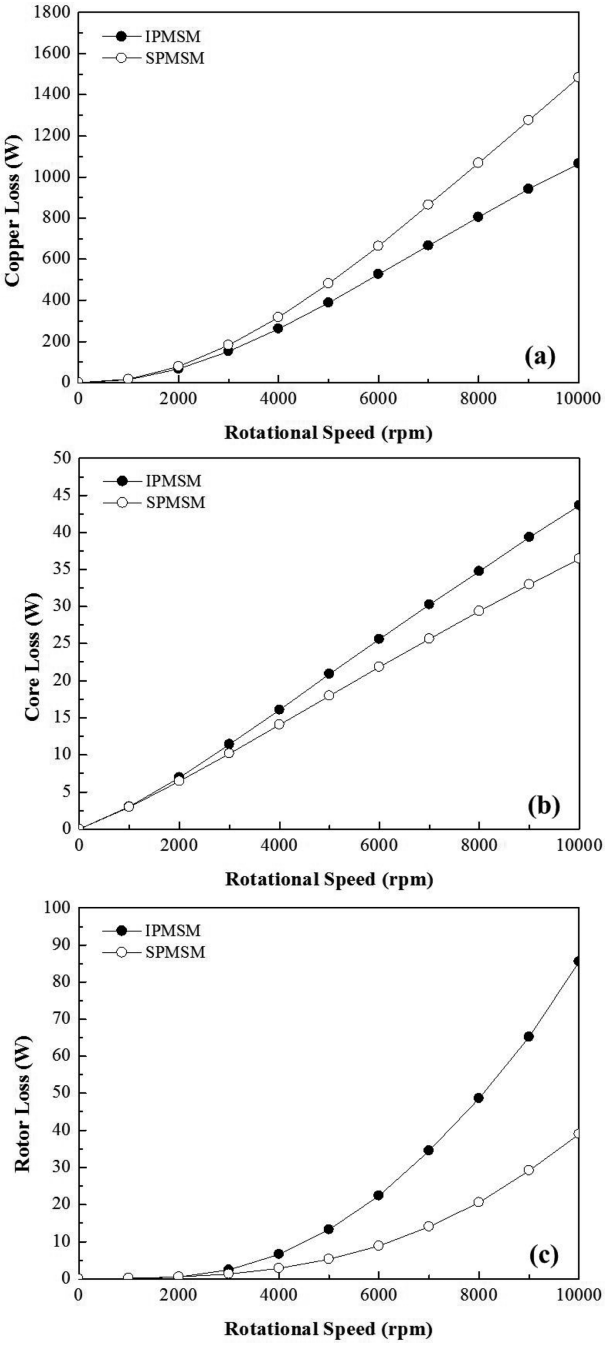

Fig. 18. Power loss characteristics according to rotational speed in generating mode: (a) copper loss, (b) core loss, (c) rotor loss.

twice value in higher rotational speed due to relatively smaller air-gap value.

4. Conclusion

In this paper, comparative investigation on IPMSM and SPMSM is performed by considering the operating conditions. For the reasonable comparison, the machines have identical machine size and almost similar equivalent circuit parameters. In addition, for the power loss calculation, the harmonic components in the phase current are considered for more accurate analysis. On the other hand, for the experimental verification, one of the analysis models is manufactured, and the measured waveforms show well corresponded results by demonstrating the validity of the analysis result. With specific machine conditions dealt with in this paper, it can be confirmed that the SPMSM is more appropriate decision to anticipate better core loss and rotor loss characteristics.

Acknowledgment

This was supported by Korea National University of Transportation in 2017, and this work was supported by the National Research Foundation of Korea (NRF) grant funded by the Korea government (MSIP; Ministry of Science, ICT & Future Planning) (No. 2017R1C1B5015907).

References

[1] J. Ikram, N. Khan, Q. Junaid, S. Khaliq, and B. I. Kwon, J. Magn. **22**, 257 (2017).
[2] S. I. Kim and J. P. Hong, J. Magn. **21**, 405 (2016).
[3] J. H. Yoo and T. U. Jung, J. Magn. **21**, 249 (2016).
[4] H. Chen, R. Qu, J. Li, and D. Li, IEEE Trans. Magn. **51**, 8205804 (2015).
[5] A. Sun, J. Li, R. Qu, and D. Li, IEEE Trans. Magn. **50**, 8105404 (2014).
[6] K. J. Ko, S. M. Jang, J. H. Park, H. W. Cho, and D. J. You, IEEE Trans. Magn. **47**, 3292 (2012).
[7] S. M. Jang, H. K. Kim, J. Y. Choi, and K. J. Ko, J. Appl. Phys. **105**, 07F109 (2009).